

2. K. A. Lur'e, "Some problems of optimal bending and stretching of elastic plates," *Izv. Akad. Nauk SSSR, Mekh. Tverd. Tela*, No. 6 (1979).
3. A. Yu. Ishlinskii, "General theory of plasticity with linear hardening," *Ukr. Mat. Zh. Akad. Nauk Ukr. SSR*, 6, No. 3 (1954).
4. Yu. I. Kadashevich and V. V. Novozhilov, "Theory of plasticity, taking into account the residual microstresses," *Prikl. Mat. Mekh.*, 22, No. 1 (1958).
5. S. A. Khristianovich and E. I. Shemyakin, "Plane deformation of plastic material with complex loading," *Izv. Akad. Nauk SSSR, Mekh. Tverd. Tela*, No. 5 (1969).
6. A. I. Imamutdinov, "Plastic deformation of materials with complex loading," *Zh. Prikl. Mekh. Tekh. Fiz.*, No. 4 (1979).

## FLEXURAL-GRAVITATIONAL WAVES FROM MOVING DISTURBANCES

A. E. Bukatov, L. V. Cherkosov, and A. A. Yaroshenko

UDC 532.593:539.3

We investigate propagating flexural-gravitational waves, generated under the action of a load moving over the surface of a floating elastic plate, found in a state of uniform extension or compression. Without account of extension or compression stresses, flexural-gravitational propagating waves were considered in [1, 2]. Planar waves were investigated in [3, 4] under conditions of longitudinal compression.

1. Let a thin, isotropic, elastic plate float on the surface of an ideal, incompressible liquid of finite depth  $H$ . The plate and the liquid are not restricted in their horizontal stresses. The plate is displaced across the surface with a velocity  $v$  of the loading  $p = p_0 f(x_1, y)$ ,  $x_1 = x + vt$ . Consider the effect of a uniform extension on the generated flexural-gravitational marine wave, assuming that the liquid motion is a potential flow, and that the velocities of the liquid particle motion and of the plate deflection  $\zeta$  are low.

Taking into account uniform extension [5-7] in a coordinate system  $x_1, y$ , related to the moving pressure region, the problem reduces to solving the Laplace equation for the velocity potential  $\varphi$

$$\Delta\varphi = 0, \quad -H < z < 0, \quad -\infty < x, y < \infty \quad (1.1)$$

with boundary conditions

$$D_1 \nabla^4 \zeta - Q_1 \Delta_1 \zeta + \kappa_1 v^2 \frac{\partial^2 \zeta}{\partial x^2} + \zeta + \frac{v}{g} \frac{\partial \varphi}{\partial x} = -p_1 f(x, y) \quad \text{at } z=0, \quad (1.2)$$

$$\frac{\partial \varphi}{\partial z} = 0 \quad \text{at } z = -H,$$

where

$$D_1 = D/\rho g, \quad Q_1 = Q/\rho g, \quad \kappa_1 = \rho_1 h/\rho g, \quad D = Eh^3/[12(1-\mu^2)], \quad p_1 = p_0/\rho g,$$

$$\nabla^4 = \Delta_1^2, \quad \Delta_1 = \partial^2/\partial x^2 + \partial^2/\partial y^2,$$

$\rho$ , liquid density;  $E$ ,  $h$ ,  $\rho_1$ , and  $\mu$ , respectively, the normal elastic modulus, the width, density, and Poisson coefficient of the plate;  $Q$ , extension stress;  $\zeta$  and  $\varphi$ , related by the mathematical condition  $\varphi_z = v\zeta_x$  at  $z = 0$ . From here on the subscript 1 of  $x_1$  will be omitted.

Applying a Fourier transform in horizontal coordinates to solve the problem (1.1), (1.2), we obtain, in the case of an axisymmetric load, an integral representation for the plate deflection (raising the plate-liquid surface):

$$\zeta = \frac{1}{2\pi} p_1 \operatorname{Re} \left\{ \int_0^\infty \frac{r}{r} \bar{f}(r) M(r) J(r, R, \gamma) dr \right\}; \quad (1.3)$$

---

Sevastopol'. Translated from *Zhurnal Prikladnoi Mekhaniki i Tekhnicheskoi Fiziki*, No. 2, pp. 151-157, March-April, 1984. Original article submitted December 24, 1982.

$$J = \frac{1}{2\pi} \int_{-\pi/2}^{3\pi/2} \frac{1}{k_0} \exp [irR \cos (\theta - \gamma)] d\theta, \quad (1.4)$$

where  $M(r) = rg(1 + \kappa_1 rg \tanh rH)^{-1} \tanh rH$ ,  $k_0 = rv \cos \theta - \tau$ ,  $\tau = [(1 + Q_1 r^2 + D_1 r^4)M(r)]^{1/2}$ ,  $r = (m^2 + n^2)^{1/2}$ ,  $x = R \cos \gamma$ ,  $y = R \sin \gamma$ ,  $m = r \cos \theta$ ,  $n = r \sin \theta$ ,  $R = (x^2 + y^2)^{1/2}$ ,  $\bar{f}(r)$  is the Fourier transform of the function  $f(R)$ .

Consider three regions of variation of the displacement velocity of the disturbance region:

$$0 < v < v_0, \quad v_0 < v < \sqrt{gH}, \quad v > \sqrt{gH}.$$

The integrand in (1.4) has for  $0 < v < v_0$  no singularities on the path of integration and, under the conditions  $v_0 < v < \sqrt{gH}$ ,  $r_1 \leq r \leq r_2$  or  $v > \sqrt{gH}$ ,  $0 < r < r_2$  has poles  $\theta_{1,2} = \mp \arccos \tau_0$ . Here,  $\tau_0 = (rv)^{-1}\tau$ ,  $v_0 = \tau(r_0)/r_0$ , where  $r_0$  is the unique positive root of the equation  $\tau'_0(r) = 0$ , the prime denotes differentiation with respect to  $r$ , and  $r_{1,2}$  are the real roots of the equation  $\tau_0(r) = 1$ . In this case,  $\tau'_0 < 0$  for  $0 < r < r_0$  and  $\tau'_0 > 0$  for  $r_0 < r < \infty$ . Besides,  $\tau_0(0) = \sqrt{gH}/v$ ,  $\lim_{r \rightarrow \infty} \tau_0 = \infty$ ,  $\tau'_0(0) = \tau'_0(r_0) = 0$ . In the case  $rH \gg 1$ ,

$$v_0 = \sqrt{g/r_0} [(1 + Q_1 r_0^2 + D_1 r_0^4)/(1 + \kappa_1 r_0 g)]^{1/2}, \quad (1.5)$$

where  $r_0$  is the positive root of the equation

$$2\kappa_1 g D_1 r^5 + 3D_1 r^4 + Q_1 r^2 - 2\kappa_1 r g - 1 = 0.$$

If  $rH \ll 1$ , then

$$v_0 = \sqrt{gH} [(1 + Q_1 r_0^2 + D_1 r_0^4)/(1 + \kappa_1 g H r_0^2)]^{1/2}, \quad (1.6)$$

and  $r_0$  satisfies the equation

$$\kappa_1 g H D_1 r^4 + 2D_1 r^2 + Q_1 - \kappa_1 g H = 0.$$

Satisfying the condition of [8], we choose the path of integration in (1.4) on the contour  $L$ , traversing on the real axis from  $\theta = -\pi/2$  to  $\theta = 3\pi/2$  with bypass points  $\theta = \theta_1$  and  $\theta = \theta_2$  in the complex  $\theta$  plane with small semicircles below and above, respectively.

2. If  $0 < v < v_0$ , applying to (1.4) the stationary-phase method and integrating consequently (1.3) by parts, we obtain that  $\zeta$  has for large  $R$  order not lower than  $O(R^{-1})$ .

Let  $v_0 < v < \sqrt{gH}$ . In this case we represent integral (1.3) in the form of a sum of three integrals over the intervals  $[0, r_1]$ ,  $[r_1, r_2]$ ,  $[r_2, \infty]$ . Since the integrand in (1.4) has no singularities on the segments  $[0, r_1]$ ,  $[r_2, \infty]$ , subsequent application of the stationary phase method and integration by parts shows that the given integrals, corresponding to the first and third segments, are of order  $O(R^{-1})$ . Consequently,

$$\zeta = \frac{1}{2\pi} p_1 \operatorname{Re} \left\{ \int_{r_1}^{r_2} r \tau^{-1} \bar{f}(r) M(r) J dr \right\} + O(R^{-1}); \quad (2.1)$$

$$J = \frac{1}{2\pi} \int_L k_0^{-1} \exp [irR \cos (\theta - \gamma)] d\theta. \quad (2.2)$$

Calculating the contour integral (2.2) with account of the signs of the expressions  $\operatorname{Re}[i \cos (\theta - \gamma)]$  on the small semicircles and the bypass points  $\theta = \theta_{1,2}$ , and substituting into (2.1) the expression obtained for  $J$ , we find

$$\zeta = \frac{1}{2\pi} p_1 \operatorname{Re} \sum_{j=1}^5 \eta_j + O(R^{-1}), \quad (2.3)$$

$$\eta_1 = \int_{r_1}^{r_2} B_1 e^{iR\Phi_1} dr, \quad 0 \leq \gamma \leq \bar{\gamma}; \quad \eta_2 = \int_{r_1}^{n_1} B_1 e^{iR\Phi_1} dr, \quad \bar{\gamma} < \gamma \leq \pi;$$

$$\eta_3 = \int_{n_2}^{r_2} B_1 e^{iR\Phi_1} dr, \quad \bar{\gamma} < \gamma \leq \pi; \quad \eta_4 = \int_{n_3}^{n_4} B_2 e^{iR\Phi_2} dr, \quad 0 \leq \gamma \leq \pi - \bar{\gamma}; \quad (2.3)$$

$$\eta_5 = R^{-1/2} \int_{r_1}^{r_2} B_3 \cos(rR - \pi/4) dr; \quad r_1 < n_1 < n_2 < r_2,$$

$$B_{1,2} = ir\bar{f}(r) M(r) \tau^{-1} \left( vr \sqrt{1 - \tau_0^2} \right)^{-1}, \quad \bar{\gamma} = \pi - \text{arctg} \max \tau_1(r),$$

$$B_3 = qr\bar{f}(r) M(r) \tau^{-1}, \quad \Phi_{1,2} = r \left( \tau_0 \cos \gamma \mp \sqrt{1 - \tau_0^2} \sin \gamma \right),$$

$$q = 2 \left[ \sqrt{2\pi r} (v^2 r^2 \cos^2 \gamma - \tau^2) \right]^{-1}, \quad \tau_1 = \tau_0^{-1} (1 - \tau_0^2)^{1/2},$$

where  $n_{1,2}$  are the real roots of the equation  $\tau_1 = -\tan \gamma$ , and  $n_{3,4}$  are the real roots of the equation  $\tau_1 = \tan \gamma$ .

The phase functions  $\Phi_1$  and  $\Phi_2$  of the integrals  $\eta_2$  and  $\eta_4$  have no stationary points, while  $\eta_5 = O(R^{-1})$ . Consequently,  $\eta_2 + \eta_4 + \eta_5 = O(R^{-1})$ .

The stationary points of the phase function  $\Phi_1$  in the intervals  $\eta_1$  and  $\eta_3$  are roots of the equations

$$\text{tg} \gamma = \tau_2(r), \quad \tau_2 = (r\tau_0)' (1 - \tau_0^2)^{1/2} [1 - \tau_0 (r\tau_0)']^{-1}. \quad (2.4)$$

For  $v_0 < v < v_1$  this equation has one  $\gamma$ -dependent real root  $r = \alpha_3$  in the regions of  $r$  variations under consideration. Here,

$$v_1 = \tau_3(r_3), \quad \tau_3 = \left[ \tau_{01}^2 - \frac{(\tau_{01}')^2 r (\tau_{01} + r\tau_{01}')}{(r\tau_{01})''} \right]^{1/2},$$

where  $r_3$  is the real root of the equation  $\tau''_2(r) = 0$ ,  $r_3 < r_0$ ,  $\tau_{01} = \tau/r$ .

Equation (2.4) has one root for  $v_1 < v < \sqrt{gH}$  if  $0 < \gamma < \gamma_2$  or  $\gamma_1 < \gamma < \pi$ . We denote this root by  $\alpha_1$  in the first case and by  $\alpha_3$  in the second. If also  $v_1 < v < \sqrt{gH}$ , but  $\gamma_2 < \gamma < \gamma_1$ , then there exist three roots  $\alpha_1 < \alpha_2 < \alpha_3$ . In this case,

$$\gamma_1 = \text{arctg} \tau_2(\alpha_4), \quad \gamma_2 = \text{arctg} \tau_2(\alpha_5), \quad \alpha_1 < \alpha_4 < \alpha_2 < \alpha_5 < \alpha_3,$$

where  $\alpha_{4,5}$  are the real roots of the equation  $\tau'_2(r) = 0$ . We note that  $\alpha_1 = \alpha_4 = \alpha_2$  for  $\gamma = \gamma_1$  and  $\alpha_2 = \alpha_5 = \alpha_3$  for  $\gamma = \gamma_2$ .

Based on the analysis performed of the location of the stationary points of the phase functions of the integrals  $\eta_1$  and  $\eta_3$ , we obtain from (2.3)

$$\zeta = \zeta_3 + O(R^{-1}) \quad \text{for } 0 < |\gamma| < \pi,$$

if  $v_0 < v < v_1$ . If  $v_1 < v < \sqrt{gH}$ , then

$$\zeta = \begin{cases} \zeta_1 + O(R^{-1}) & \text{for } 0 < |\gamma| < \gamma_2, \\ \zeta_1 + \zeta_2 + \zeta_3 + O(R^{-1}) & \text{for } \gamma_2 < |\gamma| < \gamma_1, \\ \zeta_3 + O(R^{-1}) & \text{for } \gamma_1 < |\gamma| < \pi. \end{cases} \quad (2.5)$$

Here,  $\zeta_k = R^{-1/2} \psi(\alpha_k) \cos \left[ R\Phi_1(\alpha_k, \gamma) - (-1)^k \frac{\pi}{4} \right]$ ,  $\psi = -f_1(r) M(r) \left[ vr \sqrt{1 - \tau_0^2} \right]^{-1} (2\pi |\Phi_1''|)^{-1/2}$ ,  $f_1(r) = \bar{f}(r) P_1$ .

It is seen that for velocities  $v_0 < v < v_1$  of moving disturbances only one wave system  $\zeta_3$  is generated, being damped with distance as  $1/R^{1/2}$ . These waves cover the whole surface of the plate (plate-liquid boundary). The paddle direction of these waves at a large distance from the  $x$  axis is determined by the angle

$$\gamma_0 = \text{arctg} [(v/v_0)^2 - 1]^{-1/2}.$$

The distance between neighboring paddle waves on the rays  $\gamma = 0$  and  $\gamma = \pi$  equals, respectively,  $\lambda_1 = 2\pi/r_1$ ,  $\lambda_2 = 2\pi/r_2$ . The distance from the moving disturbance to the wave paddle, following the disturbance, equals  $l_1 = \pi/4r_1$ , and up to the wave paddle, traveling in advance,  $l_2 = 3\pi/4r_2$ .

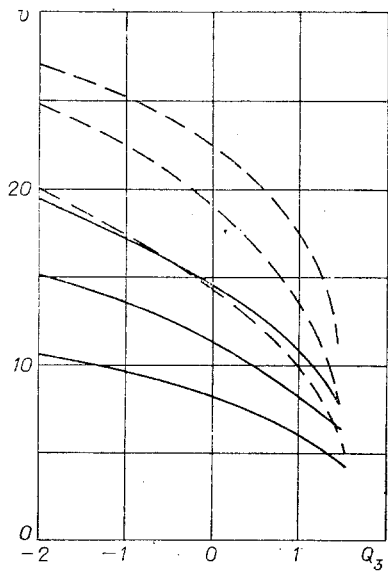


Fig. 1

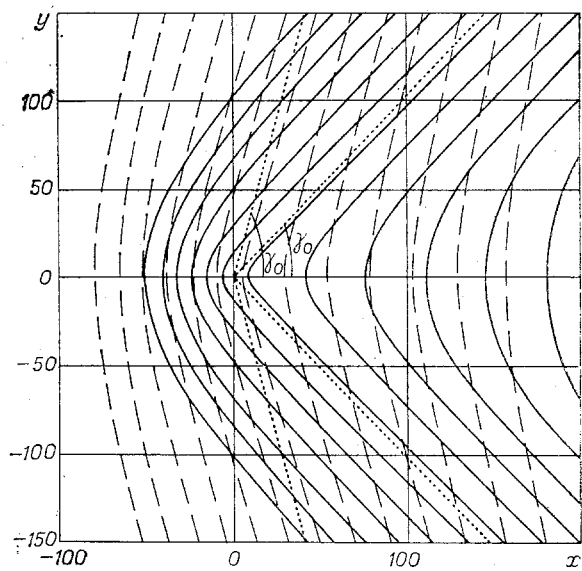


Fig. 2

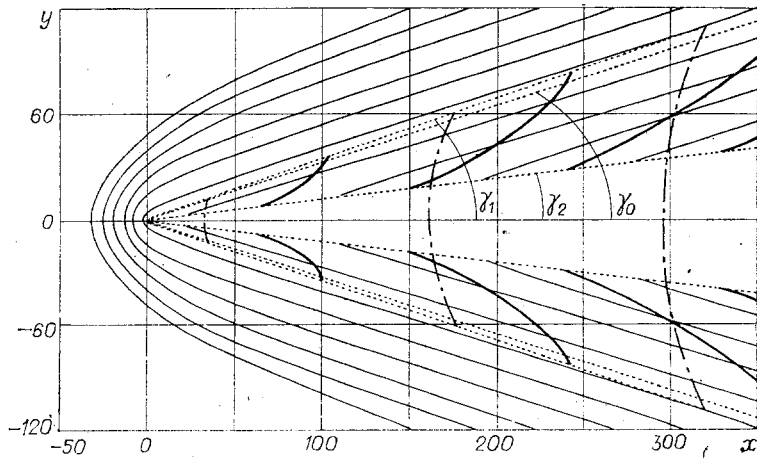


Fig. 3

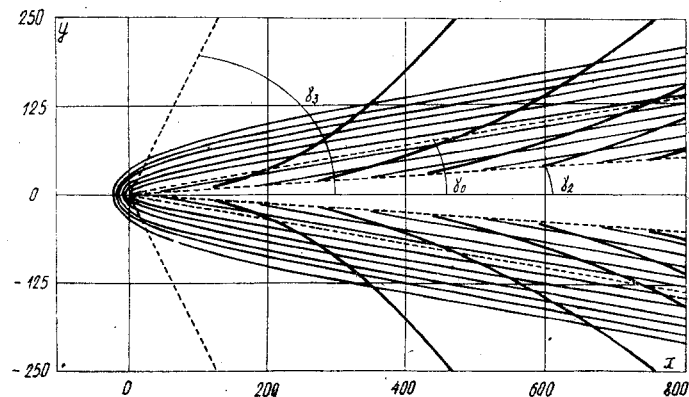


Fig. 4

Three wave systems are formed for velocities  $v_1 < v < \sqrt{gH}$ :  $\zeta_1$ ,  $\zeta_2$ , and  $\zeta_3$ . The wave system  $\zeta_1$  has the nature of transverse waves, while  $\zeta_2$  has that of longitudinal gravitational marine waves [2, 9, 10], deformed due to extensions, elastic, and mass forces on the plate. The waves  $\zeta_3$ , formed in this case in the region  $\gamma_2 < |\gamma| < \pi$ , are due, as in the case  $v_0 < v < v_1$ , to exclusively elastic plate forces, and their paddle direction is also characterized by the angle  $\gamma_0$ .

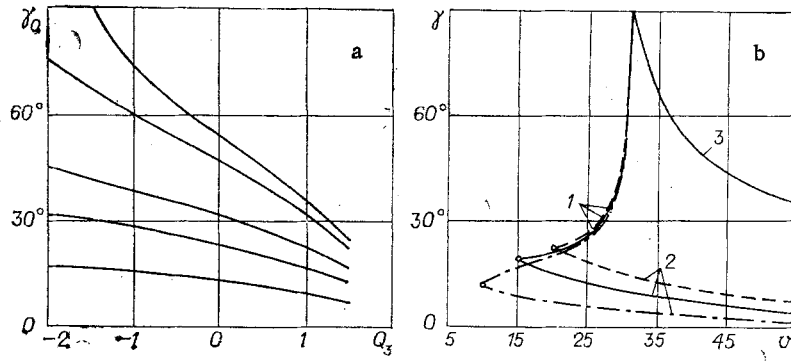


Fig. 5

Now let  $v > \sqrt{gH}$ . In this case,  $r_1 = 0$ , and the equation  $\tau'_2(r) = 0$  has only one real root  $\alpha_5$ . The phase function of the integrals  $\eta_1$  and  $\eta_3$  has for  $0 < \gamma < \gamma_2$  no stationary points, namely real roots of Eq. (2.4). For  $\gamma_2 < \gamma < \gamma_3$ , where  $\gamma_3 = \arctan[v^2(gH)^{-1} - 1]^{-1/2}$ , there are two stationary points  $\alpha_2$  and  $\alpha_3$ , and for  $\gamma_3 < \gamma < \pi$  - only one  $\alpha_3$ . Taking this into account, we find from (2.3)

$$\zeta = \begin{cases} O(R^{-1}) & \text{for } 0 < |\gamma| < \gamma_2, \\ \zeta_2 + \zeta_3 + O(R^{-1}) & \text{for } \gamma_2 < |\gamma| < \gamma_3, \\ \zeta_3 + O(R^{-1}) & \text{for } \gamma_3 < |\gamma| < \pi, \end{cases}$$

where  $\zeta_2$  and  $\zeta_3$  are the same as in (2.5).

Consequently, the disturbances displaced with velocity  $v > \sqrt{gH}$  excite two wave systems:  $\zeta_2$  and  $\zeta_3$ . The waves  $\zeta_3$  form above the angle  $\gamma < |\gamma_2|$ . Inside it, following the moving disturbances, waves with an amplitude decaying as  $1/R^{1/2}$  are generally not generated. The waves  $\zeta_2$  are generated inside the angular zone  $\gamma_2 < |\gamma| < \gamma_3$ .

3. The wave motion generated in the case of a uniformly compressed plate in the presence of a compressing stress, satisfying the equation

$$\begin{aligned} Q_1 < Q_2 = \tau_4(r_4), \\ \tau_4 &= [(1 + D_1 r^4) \tau_5(r) + 4D_1 r^4 \tau_6(r)] [\tau_5(r) + 2\tau_6(r)] r^{-2}, \\ \tau_5 &= \text{th } rH + rH \text{ ch}^{-2} rH, \quad \tau_6 = (1 + \kappa_1 r g \text{ th } rH) \text{ th } rH, \end{aligned}$$

is described by the same equation as in the case of uniform extension, if  $Q_1$  is replaced by  $-Q_1$ .

4. For quantitative estimates of the effect of uniform compression and extension on the waves generated, we performed numerical calculations in the case of an icy plate of width 0.2, 0.5, and 1 m for the parameter values [6, 11]:

$$E = 3 \cdot 10^9 \text{ N/m}^2, \quad \rho_1 = 870 \text{ kg/m}^3, \quad \mu = 0.34, \quad \rho = 10^3 \text{ kg/m}^3, \quad H = 10^2 \text{ m}. \quad (4.1)$$

The magnitude of the extension stress varied in the region  $[0.2\rho g\sqrt{D_1}]$ , and of the compressing one - in the range  $(0, \rho g Q_2)$ . Here  $Q_2$  for  $h = 0.2, 0.5, \text{ and } 1 \text{ m}$  is equal to  $1.479\sqrt{D_1}, 1.478\sqrt{D_1}, \text{ and } 1.476\sqrt{D_1}$ , respectively. The calculation results are presented in Figs. 1-6, where  $Q_3 = Q_1/\sqrt{D_1}$ . Negative  $Q_3$  values characterize extension, and positive ones - compression. The value  $Q_3 = 0$  corresponds to the case of absence of compression and extension stresses [1, 2]. The  $Q_3$ -dependence of  $v_0$  and  $v_1$  (m/sec) is illustrated in Fig. 1. The solid ( $v_0$ ) and dashed ( $v_1$ ) lines correspond, from above downward, to the plate thicknesses of 1, 0.5, and 0.2 m. It is seen that the values of the critical velocities  $v_0$  and  $v_1$ , near which the nature of the wave motion varies slowly, increase with increasing extension stresses, and decrease with increasing compression stresses. These changes may well be significant. For example, for plate thickness 1 m the values of  $v_0$  and  $v_1$  equal, respectively, 18.3 and 26.2 m/sec at  $Q_3 = -1.476, 14.6, \text{ and } 22.5$  m/sec for  $Q_3 = 0, 7.9, \text{ and } 11.0$  m/sec at  $Q_3 = 1.476$ .

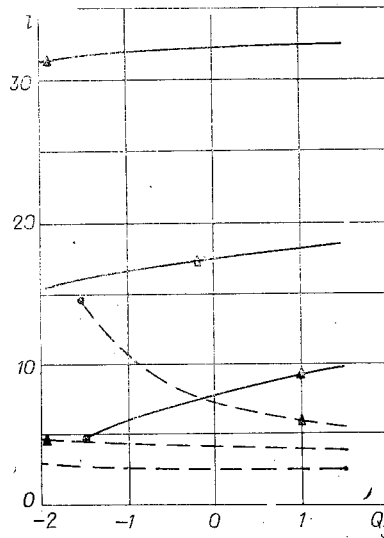


Fig. 6

The phase contours of the waves formed are illustrated in Figs. 2-4 for  $h = 0.2$  m for disturbance displacement velocities equal to 10 (Fig. 2), 20 (Fig. 3), and 35 m/sec (Fig. 4) of the regions  $v_0 < v < v_1$ ,  $v_1 < v < \sqrt{gH}$ , and  $v > \sqrt{gH}$ , respectively.

The solid ( $Q_3 = 0.5$ ) and dashed ( $Q_3 = -1$ ) curves in Fig. 2 are node lines of  $\zeta_3$  waves. The node lines of  $\zeta_3$ ,  $\zeta_2$ , and  $\zeta_1$  waves in the case  $Q_3 = 1$  correspond to the thin solid, boldface solid, and dash-dotted curves on Figs. 3 and 4. Qualitatively, the same wave patterns are also formed in the absence of compression and extension stresses ( $Q_3 = 0$ ). However, the regions of velocity variation  $v$ , for which they occur, vary with  $Q$ . The angular zone values where the  $\zeta_1$ ,  $\zeta_2$ , and  $\zeta_3$  waves are generated also change. The effect of compression and extension stresses on the value of the angle  $\gamma_0$  is characterized by the dependences shown in Fig. 5a, and on the values of the angles  $\gamma_1$ ,  $\gamma_2$ , and  $\gamma_3$  in Fig. 5b. The curve order from up downward in Fig. 5a corresponds to disturbance displacement velocities equal to 10, 11, 15, 20, and 35 m/sec. The dashed ( $Q_3 = -1.9$ ), solid ( $Q_3 = 0$ ), and dash-dotted ( $Q_3 = 1$ ) curves 1-3 correspond on Fig. 5b to the angles  $\gamma_1$ ,  $\gamma_2$ , and  $\gamma_3$ . The circles mark  $\gamma_{1,2}$  values corresponding to the velocity  $v_1$ . We note in this case that  $\gamma_1 = \gamma_3 = \pi/2$  for  $v = \sqrt{gH}$ ,  $\gamma_0 = \pi/2$  for  $v = v_0$ .

It follows from the curves given that the angle  $\gamma_0$  is larger for extension than for compression, even for  $Q_3 = 0$ . The value of the angle  $\gamma_3$  is practically independent of variations in  $Q_3$ . As to the angles  $\gamma_1$  and  $\gamma_2$ , they increase with extension stress, and decrease with increasing compression stress. Consequently, for  $v > \sqrt{gH}$  a large compression (extension) stress corresponds to a small (large) angular zone following the moving disturbances, in which the wave amplitude has an order not less than  $R^{-1}$ . The region  $\gamma_3 < |\gamma| < \gamma_2$ , where  $\zeta_2$  waves are generated simultaneously with  $\zeta_3$ , decreases for increasing extension stress, and broadens with increasing compression stress.

If  $v_0 < v < \sqrt{gH}$ , an increase in extension (compression) stress leads to a broadening (narrowing) of the formation region of transverse waves  $\zeta_1$ . In this case, the region  $\gamma_1 < |\gamma| < \gamma_2$ , in which are formed transverse  $\zeta_1$ , longitudinal  $\zeta_2$ , and flexural  $\zeta_3$  waves, decreases with increasing extension stress, and increases with increasing compression stress.

With varying  $Q_3$  the distance  $l$  along the  $x$  axis from the disturbance region to the first paddle ahead of the traveling wave  $\zeta_3$  and behind the traveling wave  $\zeta_1$  also changes. For  $h = 0.2$  m this is illustrated, respectively, by the dashed and solid lines in Fig. 6. Ordered from top downward, the solid lines correspond to disturbance displacement velocities 20, 15, and 10 m/sec, and the dashed ones — to velocities of 10, 20, and 35 m/sec. The  $l$  values marked by triangles and circles characterize the distances at which the quantity  $Q_3$  corresponds to the velocities  $v_1$  and  $v_0$ . It is seen that with increasing compressing stress the distance from the first wave paddle  $\zeta_1$  to the disturbance region increases, while with increasing extension stress it decreases. The distance from the first wave paddle  $\zeta_3$  to the disturbance region has an opposite dependence on the change in  $Q$ .

## LITERATURE CITED

1. S. F. Dotsenko, "Establishment of gravitational-elastic waves from moving disturbances," in: Tsunamis and Internal Waves [in Russian], MGI Akad. Nauk UkrSSR, Sevastopol' (1976).
2. L. V. Cherkesov, Hydrodynamic Waves [in Russian], Naukova Dumka, Kiev (1980).
3. A. E. Bukatov, "Effect of longitudinal, compressional, elastic plates on unstable wave motion of a uniform liquid," Izv. Akad. Nauk SSSR, Mekh. Zhidk. Gaza, No. 5 (1980).
4. A. E. Bukatov and V. I. Mordashev, "Effect of longitudinal, compression, elastic plates on wave disturbance development of a uniform liquid flow with a vertical shear velocity," Zh. Prikl. Mekh. Tekh. Fiz., No. 1 (1981).
5. S. Timoshenko, D. H. Young, and W. Weaver, Vibrational Problems in Engineering, 4th ed., Wiley, New York (1974).
6. D. E. Kheisin, Icecap Dynamics [in Russian], Gidrometeoizdat, Leningrad (1967).
7. M. P. Petrenko and R. P. Barsuk, "Oscillations and stability of compressed rectilinear plates on an elastic base," Prikl. Mekh., 16, No. 4 (1980).
8. J. J. Stoker, Water Waves, Interscience, New York (1957).
9. L. N. Sretenskii, Theory of Liquid Wave Motions [in Russian], Nauka, Moscow (1977).
10. L. V. Cherkesov, Hydrodynamics of Surface and Internal Waves [in Russian], Naukova Dumka, Kiev (1976).
11. V. V. Bogorodskii and V. P. Gavriilo, Physical Properties of Ice; Contemporary Methods of Glaciology [in Russian], Gidrometeoizdat, Leningrad (1980).

## CONTACT INTERACTION BETWEEN A CYLINDRICAL PANEL AND A HALF-PLANE

É. M. Kim and V. P. Ol'shanskii

UDC 539.3

## FORMULATION OF THE PROBLEM AND METHOD OF SOLUTION

Let an external load be applied to a shell and directed parallel to the edge of a semi-infinite plate, as is shown in Fig. 1. The bodies are joined in sections whose width  $h_0$  is small compared to the length  $2l$ , so that the contact domain can be considered a straight-line segment  $\{x \in [-l, l], y = 0\}$ . We take the density of the tangential contact forces  $\tau(x)$  as the principal unknown. We set the normal component equal to zero. This is justified physically by the fact that the bending stiffness of a thin-walled panel is considerably less than the tension-compression stiffness. An analogous simplification is used in [1] in analyzing the contact interaction between shells and is, in mathematical respects, that we have one singular integral equation in place of a system of two. To obtain it we take the equality of the strains  $(u_0)'_x$  in the plate and  $u'_x$  in the shell as the contact condition. Using the Green's function from [1, 2], we have

$$\int_{-l}^l \tau(\xi) \Phi(x - \xi) d\xi = f(x), \quad (1)$$

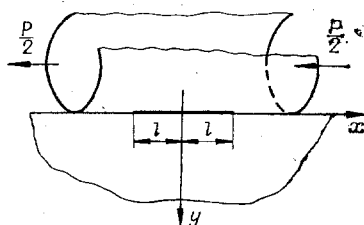


Fig. 1